TISSUE ENGINEERING: Part C
Volume 16, Number 5, 2010

DOI: 10.1089/ten.tec.2009.0394

Bioengineered Three-Dimensional Physiological Model of Colonic Longitudinal Smooth Muscle *In Vitro*

Shreya Raghavan, M.S.,[1] Mai T. Lam, Ph.D.,[2] Lesley L. Foster, B.S.,[1] Robert R. Gilmont, Ph.D.,[1] Sita Somara, Ph.D.,[1] Shuichi Takayama, Ph.D.,[2] and Khalil N. Bitar, Ph.D., AGAF[1]

Background: The objective of this study was to develop a physiological model of longitudinal smooth muscle tissue from isolated longitudinal smooth muscle cells arranged in the longitudinal axis.
Methods: Longitudinal smooth muscle cells from rabbit sigmoid colon were isolated and expanded in culture. Cells were seeded at high densities onto laminin-coated Sylgard surfaces with defined wavy microtopographies. A highly aligned cell sheet was formed, to which addition of fibrin resulted in delamination.
Results: (1) Acetylcholine (ACh) induced a dose-dependent, rapid, and sustained force generation. (2) Absence of extracellular calcium attenuated the magnitude and sustainability of ACh-induced force by 50% and 60%, respectively. (3) Vasoactive intestinal peptide also attenuated the magnitude and sustainability of ACh-induced force by 40% and 60%, respectively. These data were similar to force generated by longitudinal tissue. (4) Bioengineered constructs also maintained smooth muscle phenotype and calcium-dependence characteristics.
Summary: This is a novel physiologically relevant *in vitro* three-dimensional model of colonic longitudinal smooth muscle tissue. Bioengineered three-dimensional longitudinal smooth muscle presents the ability to generate force, and respond to contractile agonists and relaxant peptides similar to native longitudinal tissue. This model has potential applications to investigate the underlying pathophysiology of dysfunctional colonic motility. It also presents as a readily implantable band-aid colonic longitudinal muscle tissue.

Introduction

Colonic motility can be severely impacted in a variety of situations ranging from idiopathic inflammatory bowel disorders to an individual's lifestyle patterns and the amounts of stress therein. Dysmotility presents itself as diarrhea and abdominal pain among other symptoms, implicating the involvement of neural circuits and smooth muscle contractility.[1–4] The colon comprises of two principal smooth muscle layers—an inner circular layer, wherein the smooth muscle cells are aligned concentrically around the lumen, and an outer longitudinal layer, wherein the smooth muscle cells run parallel to the length of the colon. The two muscle layers, along with the enteric nervous system, modulate colonic motility patterns. The muscle layers are the primary effectors of force generation in gut motility, with their specific functionality arising from their cellular organization and alignment. Contraction of the circular smooth muscle lowers the diameter of the luminal space, whereas contraction of the longitudinal smooth muscle shortens the length of the colon. Duplication of the muscle architecture has been a key aspect of developing a three-dimensional (3D) *in vitro* model of muscle layers.

In vitro 3D models aid the study of muscle layers alone in the absence of mucosa and neural inputs, eliminating the use of full-thickness muscle preparations from animal models. Three-dimensional growth milieu facilitates well-defined aggregation geometries, mimics cellular organization *in vivo*, and thus displays functional superiority.[5,6] Structure can be directly related to function in 3D models, which is of particular importance while engineering smooth muscle tissue for force analyses.

Three-dimensional primary muscle cultures were initially reported with muscle cells bioengineered with the aid of scaffolds.[7,8] Over the years, the limitations of scaffold-based muscle tissue engineering were recognized and extensive efforts by many others were made to bioengineer self-organizing skeletal muscle constructs, vascular constructs, cardiac pressure constructs, and the like.[9–14]

We modified the model described by Dennis and Kosnik[13] for mammalian skeletal muscle constructs to culture 3D self-organizing colonic longitudinal smooth muscle tissue. We

[1]GI Molecular Motors Lab, Department of Pediatrics-Gastroenterology, University of Michigan Medical School, Ann Arbor, Michigan.
[2]Department of Biomedical Engineering, University of Michigan, Ann Arbor, Michigan.

provided a passive laminin-coated adhesion surface with microtopographies to promote cellular adhesion and orientation as described by Lam *et al.*[15,16] A 10 cm^2 cell sheet was formed with longitudinal smooth muscle cells (LSMCs) aligned along their longitudinal axis, similar to the alignment of LSMCs *in vivo*. For ease of force measurement, the oriented cell sheet was overlaid with a fibrin matrix. This coincided with the delamination and formation of bioengineered longitudinal smooth muscle tissue in ~7–10 days. Bioengineered tissue retained their physiological properties of force development and agonist-induced contractions and relaxations like native longitudinal smooth muscle tissue.

This is the first report of *in vitro* 3D culture of isolated colonic longitudinal smooth muscle without mucosal or neuronal cells. Since the bioengineered tissue is from dispersed cells that are electrically uncoupled, the study of spontaneous contractile activity of this muscle layer and its responses to peptide neurotransmitters, contractile agonists without the submucosal, and mucosal inputs, if any, is possible. Previously, longitudinal muscle activity was studied by immobilizing the adjacent circular muscle layers in flat-sheet tissue preparations, or by implanting strain gauge transducers with their measurement axis aligned to the axes of the muscle in a surgical procedure *in vivo.* These aligned constructs could be conveniently hooked to a force transducer, to effect *in vitro* force measurements *sans* a surgical procedure.

Apart from the convenience of force analysis and smooth muscle contractility studies using the 3D construct, the cells that make up the construct could also be mutated with gene therapy and/or signal transduction pathway targets. Emerging evidence suggests that modulation and control of the signal transduction pathways at the thin and thick filament levels in smooth muscles could alter the contractility of the smooth muscle.[17–19] Thus, bioengineered tissue could be a convenient 3D, physiologically relevant *in vitro* tissue engineering model to study motility-related symptomatic defects at the smooth muscle level.

Materials and Methods

Reagents

All tissue culture reagents, including basal Dulbecco's modified Eagle's medium (DMEM), fetal bovine serum (FBS), medium supplements like L-glutamine, and antibiotics, were purchased from Invitrogen (Carlsbad, CA). Acetylcholine (ACh) and vasoactive intestinal peptide (VIP) were purchased from Sigma (St. Louis, MO). Collagenase type II was purchased from Worthington (Lakewood, NJ). Sylgard [poly(dimethylsiloxane); PDMS] was from World Precision Instruments (Sarasota, FL), and Epo-Tek Resin was from Epoxy Technology (Boston, MA).

Isolation and culture of rabbit LSMCs

Rabbit sigmoid colon was removed by dissection, and relieved of fecal content. The tissue was kept on ice and moist with Hank's balanced salt solution (HBSS) containing antibiotics and sodium bicarbonate. The cleaned colon was slipped onto a plastic pipette. Blood vessels and adherent fat were picked off with forceps. Kimwipe® (Kimberly-Clark, Neenah, WI) wetted with HBSS was used to wipe the outer layer of the colon. Fine-tip forceps were used to pick off the longitudinal muscle layer from the colon and store them in ice-cold HBSS. The tissue was finely minced, digested twice with type II collagenase (0.1%) at 32°C for 1 h, and filtered through a 500-μm Nytex® (Tetko, Elmsford, NY) mesh. The filtrate was washed three times and plated in DMEM with 10% FBS, 1.5% antibiotics, and 0.5% L-glutamine onto regular tissue culture flasks.

Preparation of replicating wavy molds

Master molds with sinusoidal wavy patterns were produced by thermal expansion, oxidation, and cooling of PDMS as described by Lam *et al.*[15] Briefly, 15:1 prepolymer:curing agent by weight was wrapped around a glass cylinder with a 2 cm diameter. On plasma oxidation with air at 60 mTorr for 5–45 min, master molds with wavy patterns 6 μm apart with depths of 1700 nm were prepared.[15]

Replicating molds were made by pouring Sylgard into 60 mm plates, to a depth of 3 mm. After oven curing overnight at 60°C, a rectangular portion was cut out in the middle of the plate and discarded. Epo-Tek was poured into the plate to fill the cut-out section, and the master wavy mold was placed wave-down and UV cured.

Preparation of wavy plates for cell culture

About 10:1 Sylgard was poured into the Epo-Tek replicating mold, and cured at room temperature for 2 days. The rectangular section was then cut out, and a 35-mm-diameter hole was punched out from it to fit regular 35 mm culture plates. The round-cut wavy substrates were fixed to 35 mm plates with the wavy surface facing upward. This arrangement was left to cure and detoxify at room temperature. After 2 days, the wavy plates were sterilized under UV light and by ethanol for up to 90 min. About 2 $\mu g/cm^2$ of laminin was deposited evenly onto the tissue culture plate. Silk suture anchors, 6 mm wide, were dipped in dilute laminin solution, and were pinned onto the wavy plates, 12 mm apart. Two milliliters of the growth medium (GM; DMEM + 10% FBS, 1% Antibiotics/Antimycotic [ABAM]) was added to the plate, and stored in the incubator under sterile conditions till the cells were ready to be plated.

Bioengineering aligned cell sheets

Rabbit LSMCs (RLSMCs) were grown till they were 80–90% confluent. Cells were trypsinized as per a regular passage. About 500,000–600,000 cells are added to each wavy plate in 1.5 mL of GM and allowed to adhere and align along the wavy micropatterns on the laminin-coated PDMS substrate for 3–4 days. Once the formation of the oriented cell sheet was microscopically confirmed, 4 mg of fibrinogen, 5 units of thrombin, and GM were added. When the cell sheet began to delaminate, the GM was switched to the differentiation medium (medium 199, 5% horse serum, and 1% antibiotics) to promote smooth muscle differentiation. The aligned cell sheet delaminated and compacted, 2–4 days after gel addition, to form bioengineered longitudinal smooth muscle tissue, anchored to the two silk sutures.

Immunofluorescence

Colonic LSMCs isolated from primary cultures were grown to confluence on microscope chamber slides and treated with the differentiation medium for 2 days. Cells were then fixed and assayed with antibodies for α-smooth muscle actin (F3777; Sigma), smooth muscle specific heavy Caldesmon (c-4562; Sigma), and c-Kit (sc-168; Santa Cruz Biotechnology, Santa Cruz, CA). Negative control treatment was with secondary antibody only. Immunofluorescence was observed with an Olympus IX71 fluorescence microscope (Center Valley, PA).

Physiological testing protocols

The physiological functionality of the aligned bioengineered RLSMC tissue was evaluated in terms of force responses to various contractile agonists and antagonists. Force measurements were carried out with a custom-built magnetoresistive force transducer with an attached vernier control. An insect pin was fixed at the center of the 4 mL tissue bath, to provide a hooking point. The complete setup was housed in a vibration-resistant table.

Once the aligned cell sheets were formed, the holding pins were removed. The silk suture anchors were gently teased away from the bioengineered tissue. One end of the construct was hooked onto the movable sensing arm of the transducer, while the other end hooked onto the stationary pin. It was ensured that the tissue remained immersed in fluid, along with the mounting pins, to avoid any air vibrations. For tissue experiments, a 1 cm piece of longitudinal tissue was isolated from the rabbit colon and directly tested in the presence of tetrodotoxin.

The tissue was immersed in warm, oxygenated basal DMEM in regular calcium experiments. In zero calcium experiments, the bath medium was replaced with phosphate-buffered saline with 2 mM ethylene glycol tetraacetic acid (EGTA). A 10% stretch was applied on the constructs by the micromanipulator and this remained the length at which all further tests were carried out. The baseline of force established upon equilibration at this length was arbitrarily set to zero.

The substances used were ACh for cholinergic stimulation, and VIP. The volume of these agonists was maintained uniform at 100 μL, avoiding any error from a nonuniform diffusion of the substance. It was also noted that it took up to 60 s for the uniform diffusion of the agonists in the tissue bath. Passive tension was determined by measuring force with warmed basal DMEM alone without hooking the tissue. To determine the signal-to-noise ratio, the bioengineered tissue was attached to the measurement system without any stretch. For all other physiological force measurements, the tissue was stretched an additional 10% of its original length. Baseline was established before addition of any agonists. At the end of each experiment, or after 30 min (whichever was earlier), the longitudinal constructs were washed and supplied with fresh warm oxygenated basal DMEM.

Response to ACh was quantified by the addition of different doses ranging from 1 nM to 1 μM. In addition, a single dose of 1 μM was also independently tested on the constructs. To study the inhibition of force generation in the presence of VIP, the constructs were first treated with 1 μM VIP, and upon subsequent relaxation and recovery of baseline, 1 μM of ACh was added to the same tissue bath and without a wash the subsequent response was recorded.

Data analysis

Raw data were acquired using LabScribe2 (iWorx, Hanover, NH). GraphPad Prism 5.01 for Windows (GraphPad Software, San Diego CA; www.graphpad.com) was used for all further data analysis. Second-order Savitsky–Golay smoothing was applied on raw data. Values were expressed as means and standard error of the mean of four to seven experiments. Significant differences were tested using two-way analysis of variance with Bonferroni posttests to compare between means. A p-value less than 0.05 was considered significant. Signal-to-noise ratio was calculated by obtaining the ratio of mean baseline force of a nonstretched tissue over the standard deviation of the passive liquid tension. The traces of these measurements are shown in Figure 4.

Results

Bioengineering RLSM tissue

Figure 1 outlines the progression of steps involved in bioengineering RLSM tissue. Replicating wavy molds were made from Epo-Tek resin with defined wavy topographies. These surfaces are characterized elsewhere.[16] When 10:1 Sylgard was poured into these replicating molds, they cured in 2–3 days to form a square block with wavy patterns embedded on the surface in contact with the replicating molds. These cured Sylgard blocks were cut out and attached onto tissue culture plates with the wavy surface facing upward. The plates were left to cure and detoxify on the bench top for 2–3 days, and sterilized further in the biosafety cabinet with UV light and ethanol.

The micropatterns on the wavy plate were observed under a microscope, at 16× magnification as shown in Figure 2A. Once sterilized, the plates were coated with 1–2 $\mu g/cm^2$ of laminin. Silk sutures dipped in dilute laminin were pinned down using insect pins as shown in Figure 2B. At this point, the plates were ready for cells to be seeded onto them.

Figure 2C shows the cells on day 0, 90 min after they have been seeded onto the prepped wavy plates. The cells were randomly oriented and did not show any specific alignment. Laminin promoted cell adhesion to the otherwise nonadhesive Sylgard surface. Cells showed partial alignment along the longitudinal axis of the mold 70 h post initial cell seeding as seen in Figure 2C. Between 4 and 5 days post initial cell seeding, cellular alignment was complete, resulting in a 10 cm^2 cell sheet with completely aligned RLSMCs. The cell sheet formation was confirmed microscopically (Fig. 2C, day 5) before a fibrin gel was overlaid. The aligned cell sheet preferentially adhered to the hydrogel and delaminated from the Sylgard surface and compacted into a bioengineered longitudinal tissue (Fig. 2D).

Immunofluorescence

Isolated RLSMCs were treated with the differentiation medium for 2 days, and assayed by immunofluorescence to smooth muscle markers α-smooth muscle actin (Fig. 3A), and smooth-muscle-specific heavy Caldesmon (Fig. 3B). All the cells on the culture plate stained brightly positive for both

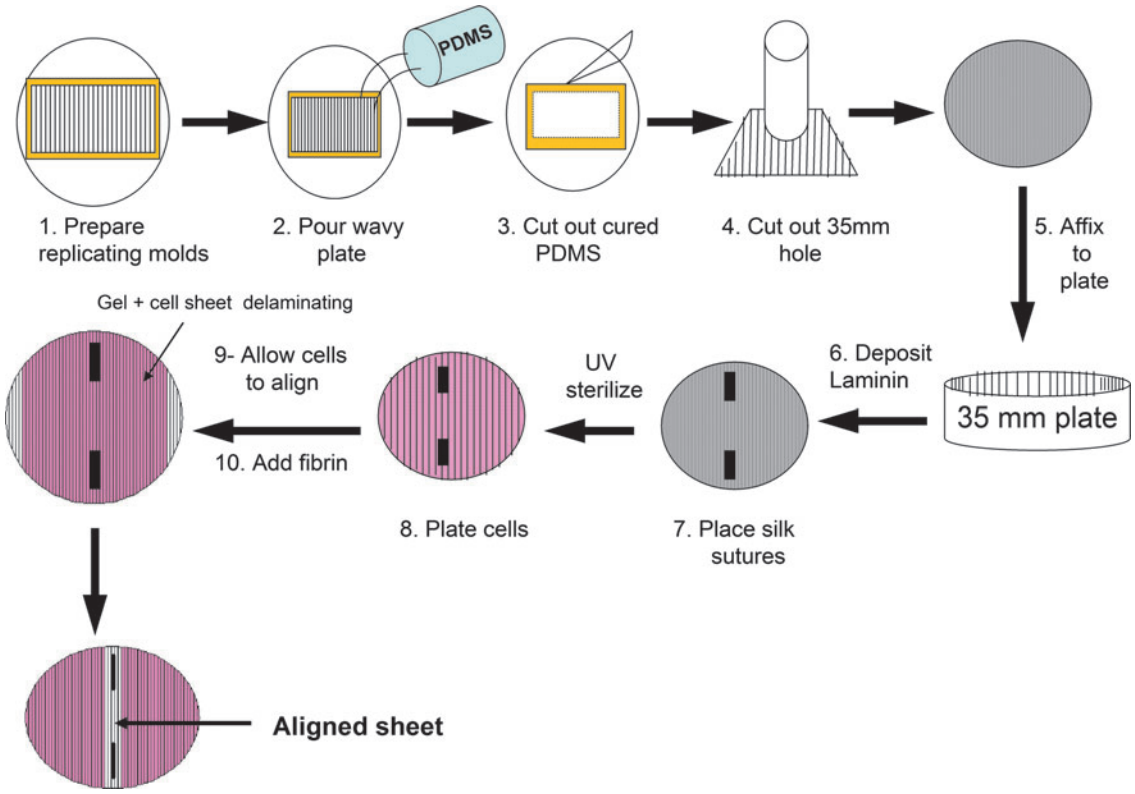

FIG. 1. Process schematic for bioengineering rabbit longitudinal smooth muscle cell (RLSMC) sheet. Replicating molds with defined wavy surfaces were patterned with Epo-Tek using thermal expansion, oxidation, and UV curing. Poly (dimethylsiloxane) (PDMS)-based wavy culture plates were cured at room temperature for at least 2 days. Circles (35 mm) were cut out from the cured PDMS and secured with more PDMS in a standard 35 mm tissue dish. The plates were sterilized and prepped for culture. Laminin is deposited onto the plate, and silk sutures are pinned down. LSMCs were cultured separately and seeded onto the plate, and allowed to align along the axis of the waves on the plate. Once alignment was microscopically confirmed (approximately 4 days postcell seeding), a fibrin hydrogel was added to promote delamination and subsequent aligned construct formation. Once alignment was microscopically confirmed (approximately 4 days postcell seeding), a fibrin hydrogel was added to promote delamination and subsequent aligned construct formation.

markers, indicating a population of smooth muscle cells. Moreover, examination of the cells for interstitial cell marker (Fig. 3C) showed a stark negative, similar to the secondary-antibody-negative control (Fig. 3D).

ACh responses in RLSM bioengineered tissue

Addition of 1 μM ACh to the tissue bath with RLSM bioengineered tissue is indicated by the arrows in Figure 5. Baseline was established before addition. Addition of a compound into the 4 mL tissue bath took up to 60 s for its uniform diffusion. The response of the bioengineered tissue (Fig. 5A) is compared to the response of native longitudinal tissue (Fig. 5B). The average force generated in a bioengineered tissue was 94.4 ± 13.244 μN ($n = 7$), while the average peak force in native tissue was 53.067 ± 5.014 ($n = 6$). Bioengineered constructs (Fig. 5A) and native tissue (Fig. 5B) both showed a rapid contraction, which was sustained for 12 min. Moreover, the tissue displayed a dose-dependent response to ACh. This property of dose dependence was maintained during the bioengineering process, as indicated by the similarity in response of the bioengineered tissue and native tissue (Fig. 6). Doses tested were between 1 nM and 1 μM.

Response to ACh in the absence of extracellular calcium

When the regular calcium medium was replaced by calcium-free phosphate-buffered saline with 2 mM chelating agent EGTA, there was a ~60% inhibition in the magnitude of peak force generated in response to 1 μM ACh. Elevated magnitudes of forces were also sustained only between 2.5 and 4 min, compared to the 12 min of sustained force in normal extracellular calcium concentrations. The bioengineered tissue preserved the property of native longitudinal smooth muscle's classical dependency on extracellular calcium.[20] Representative tracings for the trend of force generation in response to 1 μM ACh in zero calcium are shown in Figure 7 for the bioengineered tissue, as well as native longitudinal tissue.

Response to ACh post-VIP

Treatment of bioengineered RLSMC sheets, as well as native longitudinal tissue, with VIP displayed a relaxation of baseline force. Preincubation with VIP also attenuated the magnitude of force generated in response to 1 μM ACh by 40%. Bioengineered tissues generated an average peak force of 61.7 ± 8.7 μN ($n = 4$) compared to 94.4 μN generated

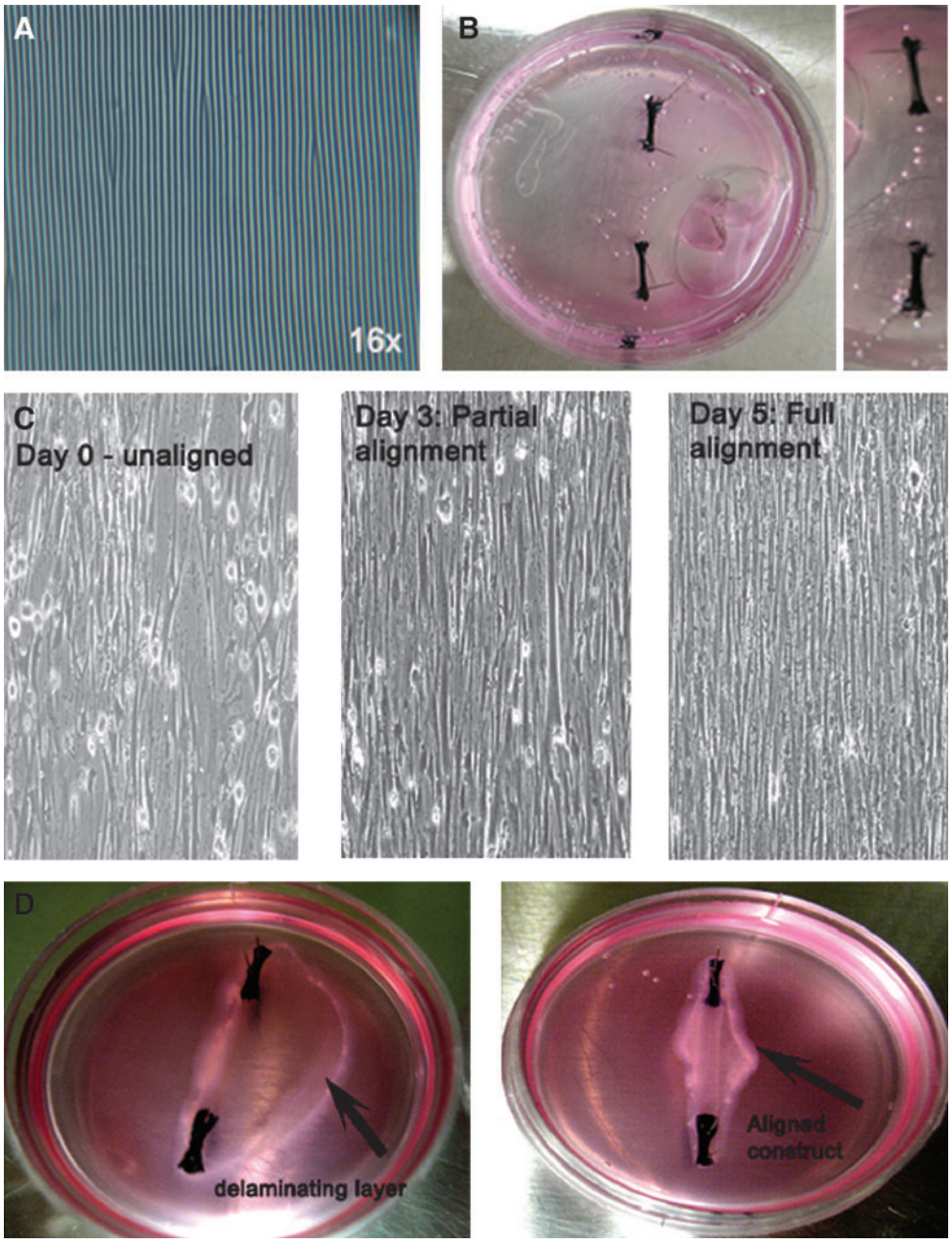

FIG. 2. Engineering highly aligned LSMC sheets. (**A**) 16× optical image of the PDMS mold fixed onto a 35 mm culture plate, with the wavy patterns seen as dark lines. (**B**) The wavy plate was functionalized with laminin, and silk sutures were pinned down 12 mm apart. The growth medium was added to the plate and left to sterilize under UV light before cells were plated onto them. (**C**) 10× inverted microscope images show that cells were unaligned 1.5 h after plating them, and show almost complete alignment on day 3. Highly aligned cell sheet formation can be seen on day 5. (**D**) Addition of the fibrin gel on day 5 promoted delamination (indicated by the black arrow), and the aligned cells contracted to form a highly longitudinally aligned construct 7 days after initial cell seeding, attached to the silk sutures.

without the VIP pretreatment. Moreover, elevated forces were also sustained only for 5 min, versus the 12 min in control ACh responses (50% inhibition). Representative traces are shown in Figure 8. A summary of the values of force generated in response to ACh under various conditions is outlined in the table accompanying Figure 9.

Discussion

The myogenic component of altered colonic motility is smooth muscle contractility. In altered motility resulting from inflammation, posttraumatic intestinal edema, and the like, the responses of circular smooth muscle layer have been characterized in detail previously. The differences in response between the circular and longitudinal smooth muscle layers have not been clearly outlined.[21–23] This presents a strong requirement for an *in vitro* model of longitudinal smooth muscle to enable the study of this muscle layer's specific contribution to abnormal colonic motility. We present a bioengineered physiologically responsive 3D reproduction of the longitudinal smooth muscle layer.

Common approaches in tissue engineering have utilized biodegradable, thermally responsive, or even nondegradable scaffolds to engineer tissues.[24] Regeneration of tissues that have a primary functionality of force development requires scaffolds that possess critical mechanical and structural properties resulting in complex and often expensive fabrication processes. Drawbacks of conventional scaffold-based tissue engineering apart from foreign body reactions also include precise control of porosity to promote cell ingrowths

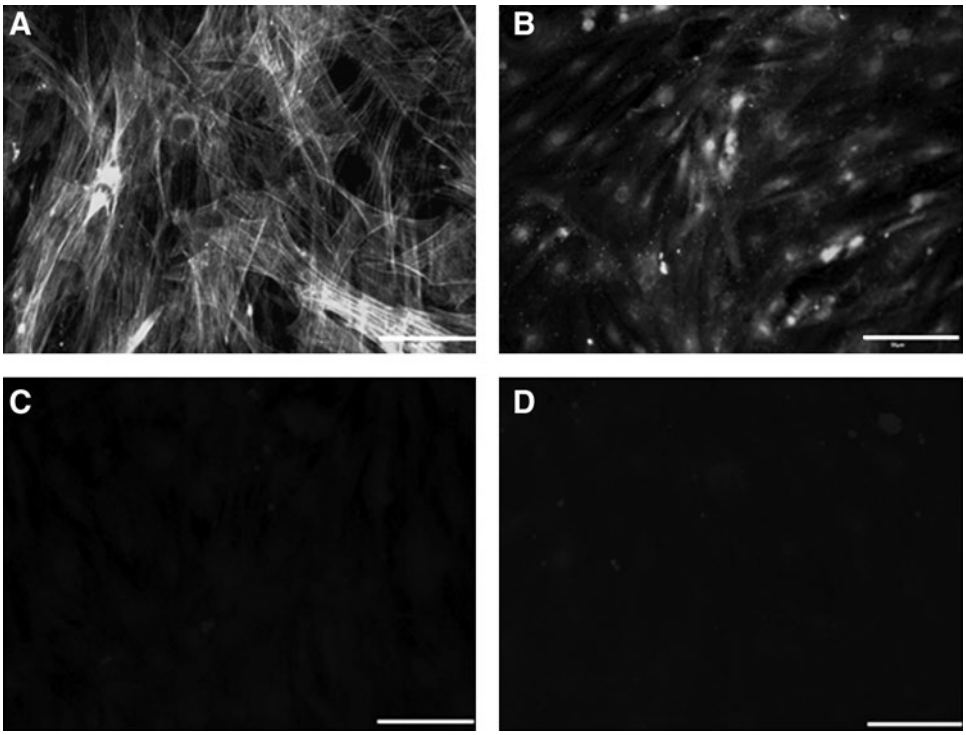

FIG. 3. Immunofluorescence on isolated RLSMC. (**A**) α-Smooth muscle actin, a smooth muscle marker, shows stained stress fibers and smooth muscle actin. (**B**) Smooth-muscle-specific heavy Caldesmon stains positive. (**C**) Interstitial cells of cajal (ICC) marker, c-Kit, shows no positive areas, indicating the absence of ICC cells in the longitudinal smooth muscle culture. (**D**) Negative control of the rabbit secondary antibody indicates weak background staining like (**C**). Scale bar = 50 μm.

and proliferation. Moreover, the use of biodegradable scaffolds present the requirement of the scaffold to have controllable degradation rates to regenerate tissue, before it degrades itself. Cells-in-gel culture techniques use extracellular matrix (ECM) solutions as natural scaffolds to promote skeletal muscle tissue regeneration, but these tissues lack physiological functionality.[25,26]

We report a physiologically functional model of longitudinal smooth muscle layer from the colon. In our method of 3D culture, we provide the LSMCs with a microtopographical surface to guide their alignment. This alignment step was important to produce a cell sheet similar to the arrangement of longitudinal smooth muscle *in vivo.* The surfaces were patterned in a reproducible and inexpensive manner using Sylgard.[15,16,27] Since cells present a lower adhesion on hydrophobic Sylgard, the surface was coated with laminin to promote cellular attachment. The surface topography aided in the alignment of the longitudinal cells to form a highly oriented cell sheet. Figure 1 outlines the various steps involved in bioengineering the cell sheet.

Original cell sheet engineering protocols used for skeletal muscle[16] were optimized to fit the culture of LSMCs. Concentrations of laminin coating the wavy plate surface and cell seeding densities were empirically determined and optimized so that the smooth muscle cells adhered long enough to align themselves along the axis of the micropatterns, mimicking alignment of LSMCs *in vivo*. We used concentrations between 1 and 2 μg/cm^2 to avoid chances of pre-

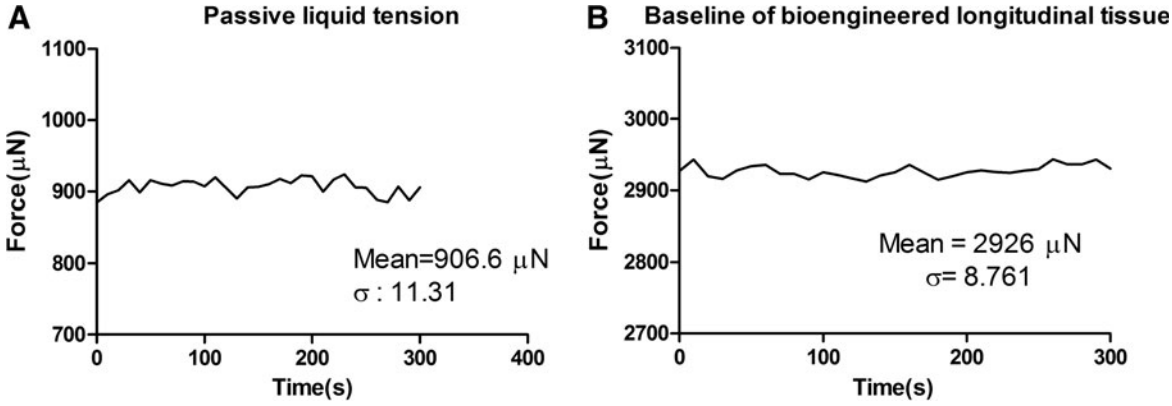

FIG. 4. Passive tension and signal-to-noise ratio (SNR). (**A**) A trace of passive tension obtained from the bath medium without tissue. To determine the degree of system noise in the measurement, the bioengineered tissue was attached to the measurement system with no external stretch. (**B**) Active tension tracing. The SNR of the system, representing the degree of active tension is the ratio of mean signal strength to the standard deviation of the noise. SNR = ~250 units.

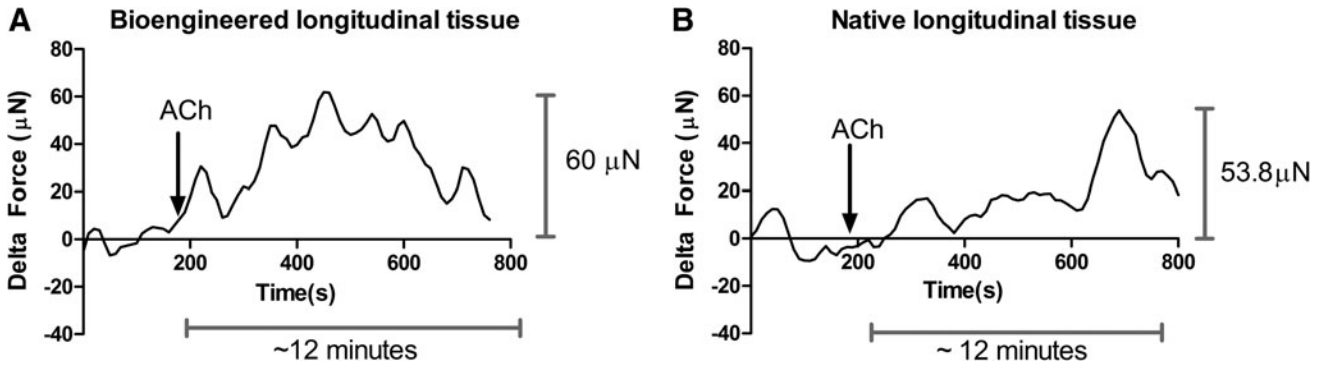

FIG. 5. Force generation in response to 1 μM acetylcholine (ACh) in (**A**) bioengineered tissue and (**B**) native longitudinal tissue. RLSMC sheets generated rapid-rising contractions of 94.4 ± 13.244 μN ($n = 7$) in response to 1 μM ACh in regular calcium media. Contractions were sustained over a 12-min period. Native longitudinal tissue also generated rapid rising contractions of 53.067 ± 5.014 ($n = 6$). Addition of ACh is indicated by the arrow at 180 s. Representative tracings for bioengineered constructs and native tissue have been chosen.

mature delamination of the longitudinal cell layer, and seeded 500,000 cells per 35 mm culture plate. The cells saturated the surface of the culture plate and there was no room for proliferation. Up to 100,000 cells were lost in medium changes when the cells were allowed to align. Over 4 days, a highly aligned cell sheet was formed, in line with the wavy Sylgard topography (Fig. 2C).

The time in culture the fibrin hydrogel was overlaid was determined empirically for different laminin concentrations. The optimal time for addition of the fibrin hydrogel was on day 4. At this point, the cells had adhered to the surface long enough to align along their longitudinal axis and had begun to delaminate. Overlaying the aligned cells with the fibrin gel coincided with the delamination, causing the cells to preferentially integrate and proliferate in the fibrin gel layer. Subsequent contraction of the fibrin gel due to inherent smooth muscle contractility and the resulting mechanical strain formed a compact LSMC sheet in 3–4 days post gel addition (Fig. 2D). Fibrin gels mimic the complexity of natural ECM and aid cell migration and ECM synthesis.[28] Functional skeletal muscle and cardiac pressure constructs were previously bioengineered using fibrin scaffolds.[10,11,29,30] The overall rate of bioengineered tissue formation depended on variables like coating laminin concentration, cell seeding density, overlaying fibrin gel concentration, and the time in culture at which the fibrin gel was overlain.

At the start of the delamination process, GM was substituted with differentiation media, primarily comprising of Medium 199 to promote the preservation of smooth muscle phenotype. Phenotype maintenance was assayed on isolated RLSM cells that were treated with the differentiation medium. The positive staining of α-smooth muscle actin and h-Caldesmon revealed that the initial populations of cells used for bioengineering maintained differentiated smooth muscle phenotype. The absence of staining with c-Kit further indicated that our initial preparation was devoid of the presence of other any other cell types, including interstitial cells of Cajal.

Bioengineered RLSMC tissues were compared with longitudinal smooth muscle tissue directly isolated from the rabbit. One-centimeter strips were chosen so as to match closely to the dimensions of the bioengineered tissues.

Bioengineered 3D RLSMC tissue responded to ACh in a functionally similar manner to longitudinal smooth muscle

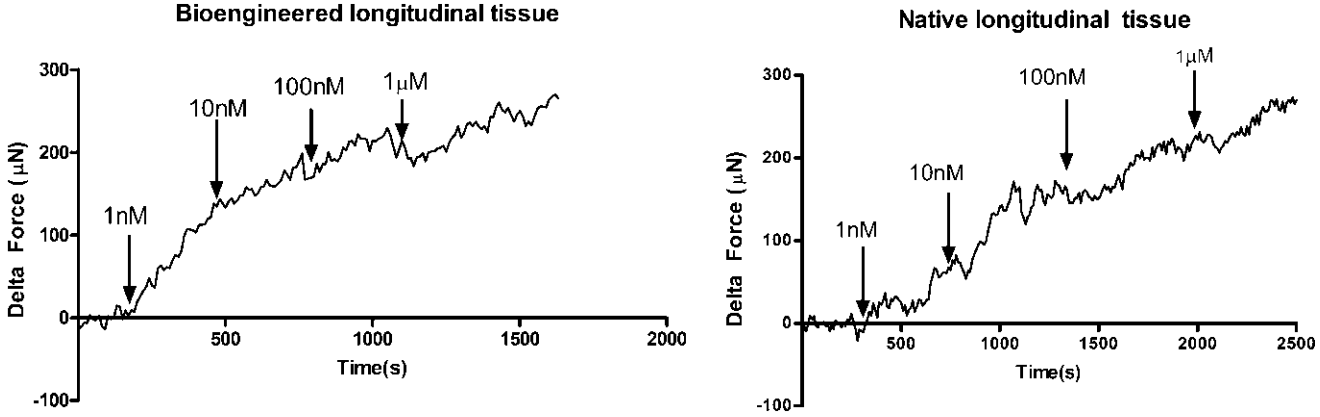

FIG. 6. Dose–response to ACh in bioengineered tissue and native longitudinal tissue. Rabbit longitudinal tissue responded to ACh in a dose-dependent manner. Doses tested were between 1 nM and 1 μM. Bioengineered sheets from isolated LSMCs retained this dose-dependence property.

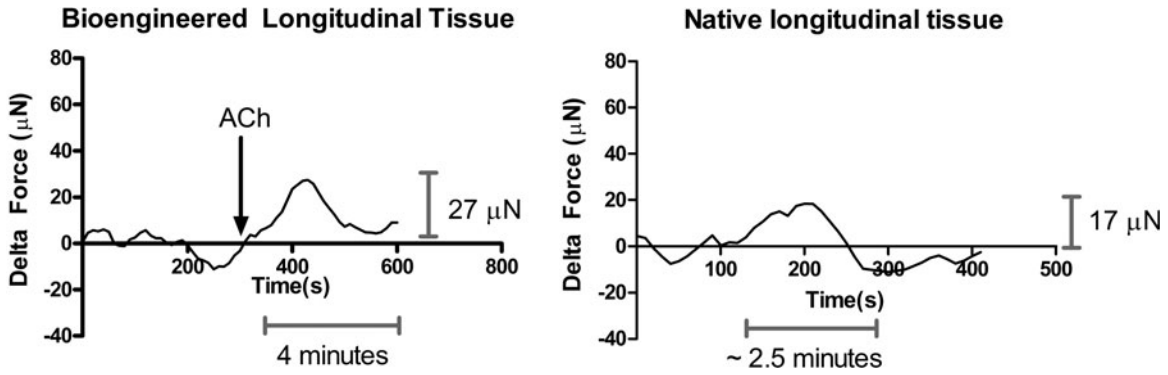

FIG. 7. Response to ACh in zero calcium in bioengineered tissue and rabbit longitudinal tissue. Native longitudinal tissue generated only $16.57 \pm 2.095\,\mu N$ ($n = 6$) in response to 1 μM ACh in the absence of extracellular calcium. This force was also sustained only for 2.5 min, versus the 12 min of force sustenance in regular calcium. Bioengineered tissue also showed force attenuated in magnitude by 50% and a reduction in time by 60%.

tissue directly isolated from the rabbit. One-micrometer ACh evoked a contractile response, generating $94.4 \pm 13.244\,\mu N$ of force (Fig. 5). Bioengineered tissue also showed dose dependency in its response to ACh, like longitudinal tissue (Fig. 6). Moreover, preincubation of the bioengineered tissue with 1 μM atropine sulfate resulted in a complete inhibition of ACh-induced contraction (data not shown). These results indicate not only that the bioengineered tissues were capable of generating force, but also that they preserved receptor-activated G-protein-mediated responses to ACh. Various biochemical pathways resulting in smooth muscle contraction in response to the contractile agonist, ACh, have been documented elsewhere,[31–34] with a commonality of downstream phosphorylation of myosin light chain and activation of protein kinase C (PKC). Bioengineered tissue also produced a rapid contraction due to membrane depolarization by 30 mM KCl and direct activation of PKC by membrane permeable phorbol ester, phorbol dibutyrate (data not shown). This demonstrates the ability of the bioengineered tissue to match the response of a native tissue.

The driving force of smooth muscle contraction is the increase in intracellular calcium concentration [Ca_i^{2+}]. Key differences between circular and longitudinal smooth muscle arise from their dependency on extracellular calcium to mobilize intracellular calcium. In longitudinal smooth muscle, agonist-induced stimulation of phospholipase A_2 and subsequent contraction requires a mandatory calcium influx step to produce calcium-induced calcium release from the sarcoplasmic reticulum mediated by ryanodine receptors.[20]

Incubation of bioengineered RLSMC tissue in zero calcium buffer with 2 mM EGTA caused it to generate a significantly lower force in response to the same concentration of ACh as before. The generation of an average force of $48 \pm 9.47\,\mu N$ (bioengineered tissue) and $16.57 \pm 2.09\,\mu N$ (native tissue) even in the absence of extracellular calcium could suggest the possible involvement of muscarinic receptor-coupled G-protein activation of phospholipase D. Phospholipase D activation has been known to mediate the hydrolysis of phosphatidylcholine, a ubiquitous phospholipid producing diacylglycerol without accompanied production of IP_3.[20] The marked absence in IP_3 production would not present any release of calcium from sarcoplasmic reticulum stores. Diacylglycerol could lead to PKC activation, thus leading to a downstream contraction in a manner that could be calcium

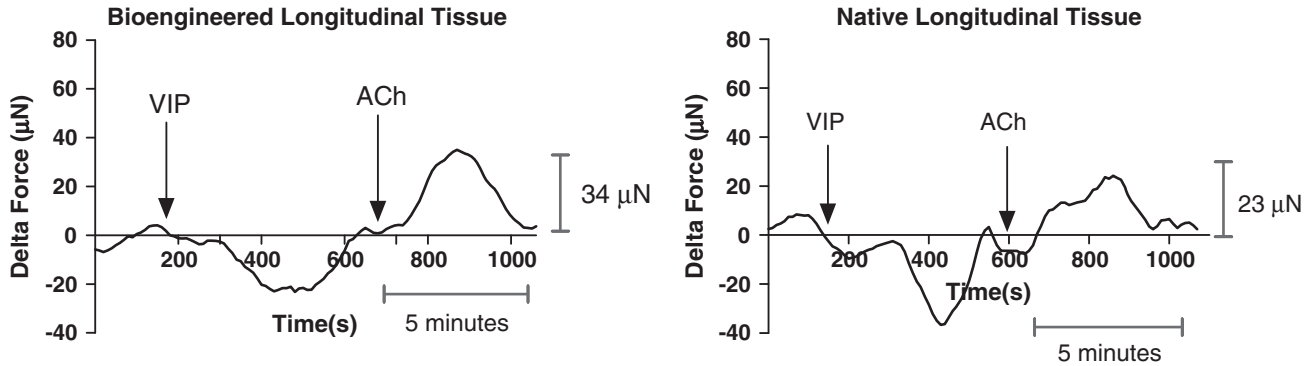

FIG. 8. Inhibition of force generation by preincubation with vasoactive intestinal peptide (VIP) in bioengineered tissue and rabbit longitudinal tissue. On treatment with VIP, both the native longitudinal tissue and the bioengineered tissue relaxed as indicated by the drop in baseline force. On subsequent stimulation with 1 μM ACh, force generated was lowered by 40% in magnitude. Force was also sustained only for 5 min, versus the 12 min of force sustenance in control ACh responses.

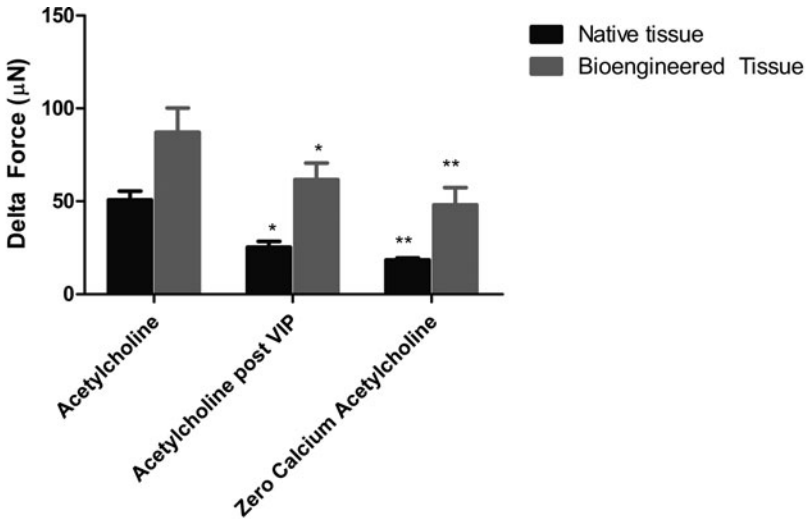

	Acetylcholine			Acetylcholine post VIP			Zero Calcium Acetylcholine		
	Mean	SEM	N	Mean	SEM	N	Mean	SEM	N
Native tissue	53.067	5.014	6	25.269	3.108	6	16.574	2.095	6
Bioengineered Tissue	94.482	13.244	7	61.719	8.788	4	48.025	9.466	4

FIG. 9. Comparison of force generated by ACh in bioengineered tissue and native longitudinal tissue. Force generation in response to ACh was significantly attenuated in magnitude and time by preincubation with VIP or in the absence of extracellular calcium. The accompanying table summarizes the mean values of force generated by the native tissue as well as the bioengineered tissue in response to 1 μM ACh under different conditions of treatment ($*p < 0.05$, $**p < 0.001$).

independent,[32,35] in response to ACh. The bioengineered tissue behaved like native tissue in its fundamental dependence on extracellular calcium.

Relaxation of LSMCs mediated by peptide neurotransmitter VIP has been well documented.[36–38] The bioengineered tissue relaxed to VIP like the native longitudinal tissue (Fig. 8). Pretreatment of bioengineered RLSMC tissue with VIP inhibited the magnitude of force generation elicited by 1 μM ACh by 40%. The initial response to ACh was still maintained even in the presence of VIP, but forces were sustained only for an overall 5 min, versus 12 min in ACh treatments that did not include a VIP pretreatment. This could indicate that VIP has a general inhibition pattern without inhibiting a specific contraction pathway, thereby not affecting the initial contraction response but producing a net overall inhibition of sustained contraction. This result is in line with previous research that shows that VIP-mediated heat shock protein-20 phosphorylation sustained over 30 min, causing relaxation and a subsequent force suppression in colonic smooth muscle cells.[17] The bioengineered tissue behaved in a functionally similar manner to native tissue in response to VIP and post-VIP ACh-induced force generation.

The physiology of the bioengineered tissue can be summarized as being responsive to receptor-mediated cholinergic (ACh) and VIP-inergic stimulation. Additionally, direct nonreceptor-mediated activation of PKC-α by phorbol ester also produced contractions. The response to potassium chloride was further testimony to the preservation of physiologically relevant membrane ion channels in the bioengineered tissue.

In conclusion, LSMC sheets have been bioengineered, allowing an extra cellular alignment step in culture, to mimic *in vivo* cellular alignment. This is the first report of a 3D colonic longitudinal smooth muscle model. The aligned cell sheet promoted the formation of essential mature cellular connections between smooth muscle cells. The cell sheet utilizes isolated longitudinal cells expanded *in vitro* using tissue culture methods. Force generation patterns revealed that bioengineered tissue responded to physiologically relevant substances like ACh and VIP in a functionally similar manner to longitudinal tissue isolated from the animal. This implies the preservation of structural receptors, for agonist-mediated G-protein-coupled contraction/relaxation pathways. Bioengineered tissues also maintain the characteristic of native longitudinal smooth muscle tissue in their dependence on extracellular calcium. The tissue-engineered cell sheet could be used as a readily implantable band-aid tissue, along with local delivery of fibroblast growth factor-2 to promote angiogenesis. This would ensure the maintenance of cell survival and tissue viability. The three-dimensionally aligned LSMC cell sheet is also a reliable *in vitro* model to study abnormal colonic motility.

Acknowledgments

This study was supported by National Institutes of Health Grant RO1 DK-057020. We thank Arti Dhiraaj for technical assistance.

Disclosure Statement

No competing financial interests exist.

References

1. Sharkey, K.A., and Kroese, A.B.A. Consequences of intestinal inflammation on the enteric nervous system: neuronal

activation induced by inflammatory mediators. Anat Rec **262,** 79, 2001.
2. Straub, R.H., Antoniou, E., Zeuner, M., Gross, V., Schölmerich, J., and Andus, T. Association of autonomic nervous hyperreflexia and systemic inflammation in patients with Crohn's disease and ulcerative colitis. J Neuroimmunol **80,** 149, 1997.
3. Collins, S.M. The immunomodulation of enteric neuromuscular function: implications for motility and inflammatory disorders. Gastroenterology **111,** 1683, 1996.
4. Vermillion, D.L., Huizinga, J.D., Riddell, R.H., and Collins, S.M. Altered small intestinal smooth muscle function in Crohn's disease. Gastroenterology **104,** 1692, 1993.
5. Mueller-Klieser, W. Three-dimensional cell cultures: from molecular mechanisms to clinical applications. Am J Physiol Cell Physiol **273,** 1109, 1997.
6. Pampaloni, F., Reynaud, E.G., and Stelzer, E.H.K. The third dimension bridges the gap between cell culture and live tissue. Nat Rev Mol Cell Biol **8,** 839, 2007.
7. Buijtenhuijs, P., Buttafoco, L., Poot, A.A., Daamen, W.F., Kuppevelt, T.H.v., Dijkstra, P.J., de Vos, R.A., Sterk, L.M., Geelkerken, B.R., Feijen, J., and Vermes, I. Tissue engineering of blood vessels: characterization of smooth-muscle cells for culturing on collagen- and elastin-based scaffolds. Biotechnol Appl Biochem **39,** 141, 2004.
8. Zimmermann, W.H., Fink, C., Kralisch, D., Remmers, U., Weil, J., and Eschenhagen, T. Three-dimensional engineered heart tissue from neonatal rat cardiac myocytes. Biotechnol Bioeng **68,** 106, 1999.
9. Dennis, R.G., Kosnik, P.E., Gilbert, M.E., and Faulkner, J.A. Excitability and contractility of skeletal muscle engineered from primary cultures and cell lines. Am J Physiol Cell Physiol **280,** C288, 2001.
10. Baar, K., Birla, R., Boluyt, M.O., Borschel, G.H., Arruda, E.M., and Dennis, R.G. Self-organization of rat cardiac cells into contractile 3-D cardiac tissue. FASEB J **19,** 275, 2004.
11. Huang, Y.-C., Dennis, R.G., Larkin, L., and Baar, K. Rapid formation of functional muscle *in vitro* using fibrin gels. J Appl Physiol **98,** 706, 2005.
12. Hecker, L., Baar, K., Dennis, R.G., and Bitar, K.N. Development of three-dimensional physiological model of the internal anal sphincter bioengineered *in vitro* from isolated smooth muscle cells. Am J Physiol Gastrointest Liver Physiol **289,** 188, 2005.
13. Dennis, R.G., and Kosnik, P.E. Excitability and isometric contractile properties of mammalian skeletal muscle constructs engineered *in vitro.* In Vitro Cell Dev Biol Anim **36,** 327, 2000.
14. Kosnik, P.E., Faulkner, J.A., and Dennis, R.G. Functional development of engineered skeletal muscle from adult and neonatal rats. Tissue Eng **7,** 573, 2001.
15. Lam, M.T., Sim, S., Zhu, X., and Takayama, S. The effect of continuous wavy micropatterns on silicone substrates on the alignment of skeletal muscle myoblasts and myotubes. Biomaterials **27,** 4340, 2006.
16. Lam, M.T., Huang, Y.-C., Birla, R.K., and Takayama, S. Microfeature guided skeletal muscle tissue engineering for highly organized 3-dimensional free-standing constructs. Biomaterials **30,** 1150, 2009.
17. Gilmont, R.R., Somara, S., and Bitar, K.N. VIP induces PKA-mediated rapid and sustained phosphorylation of HSP20. Biochem Biophys Res Commun **375,** 452, 2008.
18. Somara, S., and Bitar, K.N. Phosphorylated HSP27 modulates the association of phosphorylated caldesmon with tropomyosin in colonic smooth muscle. Am J Physiol Gastrointest Liver Physiol **291,** 630, 2006.
19. Somara, S., Pang, H., and Bitar, K.N. Agonist induced association of tropomyosin with protein kinase Cα in colonic smooth muscle. Am J Physiol Gastrointest Liver Physiol **288,** 268, 2005.
20. Murthy, K.S. Signaling for contraction and relaxation in smooth muscle of the gut. Annu Rev Physiol **68,** 345, 2005.
21. Grossi, L., McHugh, K.M., and Collins, S.M. On the specificity of altered smooth muscle function in experimental colitis in rats. Gastroenterology **104,** 1049, 1993.
22. Myers, B.S., Martin, J.S., Dempsey, D.T., Parkman, H.P., Thomas, R.M., and Ryan, J.P. Acute experimental colitis decreases colonic circular smooth muscle contractility in rats. Am J Physiol Gastrointest Liver Physiol **273,** 928, 1997.
23. Moore-Olufemi, S.D., Padalecki, J., Olufemi, S.E., Xue, H., Oliver, D.H., Radhakrishnan, R.S., Allen, S.J., Moore, F.A., Stewart, R., Laine, G.A., and Cox, C.S., Jr. Intestinal edema: effect of enteral feeding on motility and gene expression. J Surg Res **155,** 283, 2009.
24. Fedorovich, N.E., Alblas, J., Wijn, J.R.D., Hennink, W.E., Verbout, A.J., and Dhert, W.J.A. Hydrogels as extracellular matrices for skeletal tissue engineering: state-of-the-art and novel application in organ printing. Tissue Eng **13,** 1905, 2007.
25. Vandenburgh, H.H. Bioengineered muscle constructs and tissue-based therapy for cardiac disease. Prog Pediatr Cardiol **21,** 167, 2005.
26. Okano, T., and Matsuda, T. Tissue engineered skeletal muscle: preparation of highly dense, highly oriented hybrid muscular tissues. Cell Transplant **7,** 71, 1998.
27. Lam, M.T., Clem, W.C., and Takayama, S. Reversible on-demand cell alignment using reconfigurable microtopography. Biomaterials **29,** 1705, 2008.
28. Ye, Q., Zuend, G., Benedikt, P., Jockenhoevel, S., Hoerstrup, S.P., Sakyama, S., Hubbell, J.A., and Turina, M. Fibrin gel as a three dimensional matrix in cardiovascular tissue engineering. Eur J Cardiothorac Surg **17,** 587, 2000.
29. Birla, R.K., Huang, Y.-C., and Dennis, R.G. Development of a novel bioreactor for the mechanical loading of tissue-engineered heart muscle. Tissue Eng **13,** 2239, 2007.
30. Shaikh, F.M., Callanan, A., Kavanagh, E.G., Burke, P.E., Grace, P.A., and McGloughlin, T.M. Fibrin: a natural biodegradable scaffold in vascular tissue engineering. Cells Tissues Organs **188,** 333, 2008.
31. An, J.Y., Yun, H.S., Lee, Y.P., Yang, S.J., Shim, J.O., Jeong, J.H., Shin, C.Y., Kim, J.H., Kim, D.S., and Sohn, U.D. The intracellular pathway of the acetylcholine-induced contraction in cat detrusor muscle cells. Br J Pharmacol **137,** 1001, 2002.
32. Hillemeier, A.C., Deutsch, D.E., and Bitar, K.N. Signal transduction pathways associated with contraction during development of the feline gastric antrum. Gastroenterology **113,** 507, 1997.
33. Ding, X., and Murray, P.A. Acetylcholine activated protein kinase C-alpha in pulmonary venous smooth muscle. J Am Soc Anesthesiol **106,** 507, 2007.
34. Patil, S.B., and Bitar, K.N. RhoA- and PKCα-mediated phosphorylation of MYPT and its association with HSP27 in colonic smooth muscle cells. Am J Physiol Gastrointest Liver Physiol **290,** G83, 2006.

35. Schmidt, M., Huewe, S.M., Fasselt, B., Homann, D., Ruemenapp, U., Sandmann, J., and Jakobs, K.H. Mechanisms of phospholipase D stimulation by m3 muscarinic acetylcholine receptors: evidence for involvement of tyrosine phosphorylation. Eur J Biochem **225,** 667, 1994.
36. Kishi, M., Takeuchi, T., Suthamnatpong, N., Ishii, T., Nishio, H., Hata, F., and Takewaki, T. VIP- and PACAP-mediated nonadrenergic, noncholinergic inhibition in longitudinal muscle of rat distal colon: involvement of activation of charybdotoxin- and apamin-sensitive K + channels. Br J Pharmacol **119,** 623, 1996.
37. Kishi, M., Takeuchi, T., Katayama, H., Yamazaki, Y., Nishio, H., Hata, F., and Takewaki, T. Involvement of cyclic AMP–PKA pathway in VIP-induced, charybdotoxin-sensitive relaxation of longitudinal muscle of the distal colon of Wistar-ST rats. Br J Pharmacol **129,** 140, 2000.
38. Lefebvre, R.A., Smits, G.J., and Timmermans, J.P. Study of NO and VIP as non-adrenergic non-cholinergic neurotransmitters in the pig gastric fundus. Br J Pharmacol **116,** 2017, 1995.

Address correspondence to:
Khalil N. Bitar, Ph.D., AGAF
GI Molecular Motors Lab
Department of Pediatrics, Gastroenterology
University of Michigan Medical School
1150 W. Medical Center Drive
MSRB I, Room A520
Ann Arbor, MI 48109-0658

E-mail: bitar@umich.edu

Received: June 10, 2009
Accepted: December 14, 2009
Online Publication Date: February 4, 2010